

Effects of different block design on the performance of inline cross-flow turbine used in urban water mains

Du Jiyun, Shen Zhicheng, Yang Hongxing*

Renewable Energy Research Group (RERG), Department of Building Services
Engineering, The Hong Kong Polytechnic University, Hong Kong, China

Corresponding author email: Hong-xing.yang@polyu.edu.hk

Abstract

Cross-flow turbines provide a promising and cost-effective solution to hydropower harvesting from water mains for power supply to water monitoring system. However, the design method and performance of cross-flow turbines used in water mains has not been fully investigated. In this paper, a configuration of inline cross-flow turbine with two blocks is proposed and a block design method is presented. Specifically, numerical investigations are carried out to verify the proposed method and study the effect of different block design on turbine performance. Flow velocity analysis shows that the proposed block can improve the flow attack angle at the runner inlet and increase the flow velocity through the runner significantly. Besides, the pressure distribution indicates that the blocks can increase the pressure difference through the runner thus improve the turbine performance. By comparing three models with different guide block orientation angles, it is found that the model with bigger conversion block orientation angle has a better performance because the blocks from this model not only have a better function in flow separation and negative torque reduction at the first stage, but also convert more water head into kinetic energy. Numerical results show that the inline turbine could achieve its maximum efficiency of 42.4% with about 1500W power output, while the water head reduction is limited in an acceptable range.

Keywords: Water monitoring system; urban water mains; micro hydropower; inline cross-flow turbine

1. Introduction

Water is one of the main bases for residential living and social development [1]. With the continuous population increase and urban development, many cities around the world are facing great challenges in reliable and secure water supply [2]. However, a lot of fresh water is wasted in the delivery process due to leakage or pipe bursting and it is estimated that more than 32 billion m^3 water is wasted from water mains worldwide every year [3]. Taking Hong Kong for instance, nearly 1200 Mm^3 water is delivered through water pipes to the residents annually and the amount will grow to 1315 Mm^3 in 2030 [4], however, nearly 15% of fresh water was wasted in 2016 due to pipe leakage [5]. Therefore, many kinds of water monitoring sensors, including water flow sensors, pressure sensors and acoustic leakage sensors, are used along urban water mains for timely detection and early warning of water leakage [6]. However, these sensors are usually powered by traditional batteries which usually have limited lifespans even with efficient energy conserving mechanisms [7]. Once the batteries ran out, the water monitoring system would die, so the batteries need to be replaced frequently, resulting in a high cost and a huge demand for labor [8]. For this reason, renewable energies such as vibration, solar energy and wind energy have attracted growing attention as alternative sensor power sources in recent years [9] [10] [11]. However, these power sources are uncontrollable and not steadily available. Besides, their energy harvesters are usually bulky and thus need more space to install, resulting in significant restrictions to their application in water monitoring system.

Usually, excess water head exists in urban water mains to ensure constant water supply through the pipe network, so it is likely to be a promising way to harvest excess energy inside water mains and transfer it into electricity for power supply to water monitoring sensors. In our former research, the feasibility of using an inline cross-flow turbine in water supply pipes for hydropower harvesting has been studied by numerical and experimental methods [12] [13]. Figure 1 shows schematic diagram of the inline cross-flow turbine. In the proposed turbine, a DN100 T-joint is integrated

to a part of water mains, then a cross-flow runner which connects with a generator via a shaft is inserted in the pipe through the T-joint to harvest hydropower and transfer the power to the generator. After that, the generated electricity will be stored in chargeable batteries after rectification. Besides, two blocks which integrate to pipe inner wall are designed to function as ducted elements to accelerate the water flow and direct it to the runner. It is found that the blocks have significant effects on the performance of inline cross-flow turbine. However, researches about the design method are still rare, which significantly limits the performance enhancement and widespread application of the inline cross-flow turbines.

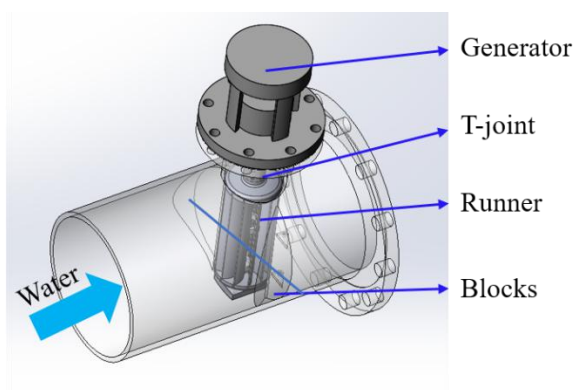


Fig.1 Schematic diagram of the inline cross-flow turbine

For conventional cross-flow turbines, nozzles are usually used as the ducted elements and large amounts of researches have been done by numerical or experimental methods for nozzle design and optimization to improve the overall performance of conventional cross-flow turbines. As the blocks in an inline cross-flow turbine has similar function with the nozzle in conventional cross-flow turbines, researches on nozzle design and optimization could provide inspirations for the blocks design. Adhikari et al. [14] developed a two-dimensional analytical model for the nozzle design of cross-flow turbines by theoretical and numerical methods, the results showed that the proposed method is effective to improve the turbine efficiency. Sammartano et al. [15] proposed a nozzle design method by adopting a linear variation of the nozzle inner wall to obtain an approximately constant attack angle

along the impeller inlet. Choi et al. [16] studied the effects of nozzle shape on the pressure and velocity distribution inside the cross-flow turbine while Chichkhede et al. [17] investigated the turbine performance at different nozzle openings by numerical methods. Acharya N. et al. [18] enhanced the performance of a cross-flow turbine by varying the nozzle shape and guide vane angle, the results indicated that the efficiency increased by 12.9% after geometrical modification. When applied in water pipes or water tunnels, the configuration of cross-flow turbine must be modified as the turbine is used submerged and the water flow will exert negative torque on the returning blades, resulting in a bad influence on the turbine performance [19]. Many investigators enhanced the performance of submerged cross-flow turbines in water tunnel by placing ducted or augmented elements around the impeller to increase flow velocity and pressure difference and shield the flow towards the returning blades [19,20,21]. Elbatran [19] developed a kind of ducted nozzle Savonius water turbine and studied the effects of nozzle shape on the turbine performance, results showed that turbine maximum power coefficient increase by 78% compared to the conventional rotor. Prasad et al. [20] investigated the performance characteristics of a cross-flow tidal turbine with bidirectional nozzles, the maximum efficiency is recorded 55%. Kim et al. [21] also studied the influence of channel area on the bidirectional cross-flow wave turbine. Elbatran et al. [22] designed a cross-flow turbine with dual directed nozzles used in channels, the simulation results indicated a maximum efficiency of 52%.

It is a promising solution for power supply to water monitoring sensors and meters using inline cross-flow turbines as a sustainable power source. Literature review indicates that the nozzle shape improvement can significantly enhance the performance of traditional cross-flow turbines. However, there is no design method for the blocks of inline cross-flow turbines, which possesses a limitation to its performance improvement and widespread application. In this paper, a mathematic design method for the block of inline cross-flow turbine is newly developed and the

influence of different block design on the performance of inline cross-flow turbine is investigated by numerical methods. The rest of the paper is organized as follows: Section 2 present the research methodology used in the research. Specifically, Section 2.1 describes the numerical method used for turbine performance prediction and flow characteristics analysis. Section 2.2 presents the hydraulic test rig and turbine prototype used for validation of numerical method. Section 2.3 describes the method used for results analysis. Section 3 presents the numerical results and relevant analysis, effect of different block design on the turbine performance and the mechanism is investigated. The main findings are summarized in Conclusion section.

2. Methodology

Figure 2 indicates the research flow chart of the study. The study starts from proposing a mathematic design method for the blocks. then the models of the inline cross-flow turbines with different block shapes are built. After that, Computational Fluid Dynamics (CFD) method which is validated by our previous experimental results is used to validate the proposed mathematic design method, predict the turbine performance and analyze the flow characteristics inside the turbine. The aim of the study is to propose an effective block design method and determine the optimal block for the inline cross-flow turbine.

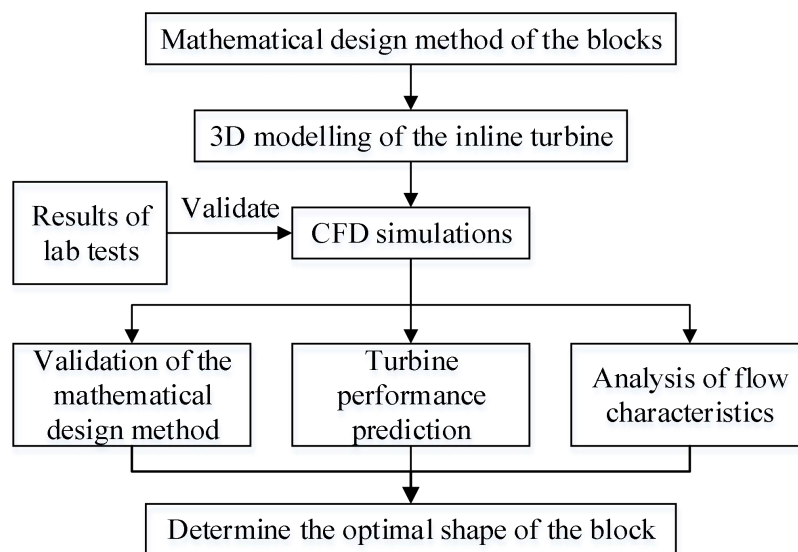


Fig.2 The research flow chart

2.1 Geometrical design of the inline turbine

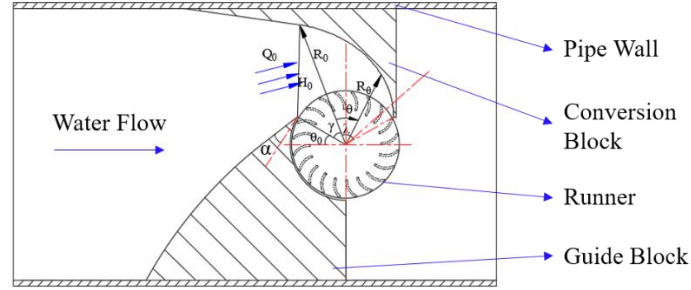


Fig.3 The turbine design scheme

The design scheme of the inline turbine is shown in Figure 3. As indicated in Figure 3, two blocks are integrated with the inner wall of the pipe inner wall, the left block is called Guide Block as its main function is to direct the water flow to the runner, while the right block is named as Conversion Block because it is used to convert part of the water head into flow kinetic energy. Besides, a cross-flow runner is inserted in the pipe through a T-joint to capture the excess energy of the water flow and transfer it to the generator. The main aim of this study is to propose a mathematic design method for the blocks.

2.1.1 Geometrical design of the blocks

As shown in Figure 3, the main aim of block design is to determine the inner wall shape $R(\theta)$ of the conversion block. To develop a method for the block design, the followed assumptions are made:

- 1) All the reduced water head is converted into flow kinetic energy.
- 2) The distribution of water flow rate at the runner inlet discharge area is uniform.
- 3) The flow velocity in the space between the conversion block and runner is uniform.

The space between the conversion block and runner can be divided into many cross sections that across $R(\theta)$ and runner central axis, based on assumption 2, the flow rate

through each cross section Q_θ can be calculated as:

$$Q_\theta = \frac{\lambda - \gamma - \theta}{\lambda} Q \quad (1)$$

where Q is the total flow rate through the runner, m³/h; λ is block entry arc angle; γ is the orientation entry angle of the conversion block; θ is the azimuthal angle of cross sections.

When $\theta = 0$, the flow rate at the inlet of conversion block is:

$$Q_{in} = \frac{\lambda - \gamma}{\lambda} Q \quad (2)$$

So, the inlet area of the conversion block A_{in} can be calculated:

$$A_{in} = \frac{Q_{in}}{V_{in}} \quad (3)$$

Based assumption 1 and energy equation, the velocity at the block inlet can be determined as:

$$g\Delta H = \frac{1}{2}(V_{in}^2 - V_0^2) \quad (4)$$

where ΔH is the water head reduction through the turbine, m; V_0 is the water flow velocity in the pipe, m/s.

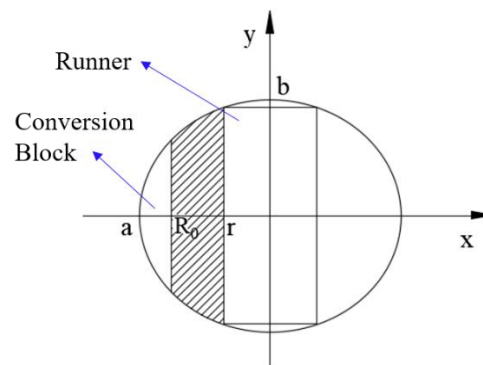


Fig.4 Diagram of cross section at the conversion block inlet

Figure 4 shows the cross section of the water pipe at the inlet of the conversion block.

In this diagram, r is the outer radius of the runner. It can be observed that the shape of

the cross section is an ellipse that can be described as:

$$\frac{x^2}{a^2} + \frac{y^2}{b^2} = 1 \quad (5)$$

$$a = R_{pipe} / \cos(\frac{\pi}{2} - \theta_0 - \gamma - \theta) \quad (6)$$

$$b = R_{pipe} \quad (7)$$

where a is the length of long axes of the ellipse, m; b is the length of short axes of the ellipse, m; R_{pipe} is the radius of the water pipe, m; θ_0 is the orientation angle of guide block.

The orientation entry angle of the conversion block can be calculated by:

$$\gamma = \csc(\frac{r \cos \theta_0}{R_0}) - \theta_0 \quad (8)$$

The cross section between the block and runner is a part of the ellipse (the shaded part in Figure 4) and its area A'_m can be calculated as:

$$A'_m = 2 \int_r^{R_0} y dx \quad (9)$$

The definite integral can be solved by substitution method:

$$A'_m = \frac{ab}{2} (\sin 2t_2 - \sin 2t_1) - ab(t_2 - t_1) \quad (10)$$

$$t_1 = \csc \frac{r}{a} \quad (11)$$

$$t_2 = \csc \frac{R_0}{a} \quad (12)$$

where, t_1 and t_2 are the substitution parameters.

It is very difficult to solve these equations directly, but the value of R_0 can be approximately obtained by iteration. Firstly, an initial value of R_0 is given, then the value of γ , A'_m and A_m can be calculated. If the value of A'_m is approximate to

A_m , e.g. $\left| \frac{A'_m - A_m}{A_m} \right| \leq 2\%$, this R_0 can be regarded as the required value. Or else,

change the value of R_0 and repeat the calculation again until the approximation condition is satisfied. After determination of the inlet geometrical shape, the shape of several intermediate cross sections can also be calculated. Finally, a three-dimensional block model can be obtained.

As the main function of guide block is to direct the water flow to the runner and conversion block. Its main geometrical parameter is the attack angle α which is showed in Figure 3. The attack angle determines the flow inlet direction and its effect on the turbine performance has been studied by several researchers [7, 23, 24, 25]. In this study, the value of attack angle is designed as 22° , which is suggested as the optimum value by the references[15, 25].

2.1.2 Geometrical parameters of the runner

Runner is another important component which captures energy from the water flow, its structure and main geometrical parameters are indicated in Figure 5. The runner consists of 20 blades and 3 discs which are used to hold the blades and reduce blades deformation. Among the runner design parameters, the length L and the outer diameter of the runner D_1 are determined by the diameters of water pipe and T-joint, respectively. As the main objective of this study is to investigate the effect of block design on turbine performance, the ratio of inner and outer diameter D_2/D_1 , outer blade angle β_1 and inner blade angle β_2 are determined based on the empirical values suggested in reference [7]. Considering the limited space and machining difficulty, the blades number N_b is selected as 20. The blade radius R_b is calculated by:

$$R_b = \frac{D_1^2 - D_2^2}{4D_1 \cos \beta_1} \quad (13)$$

The runner geometrical parameters are listed in Table 1.

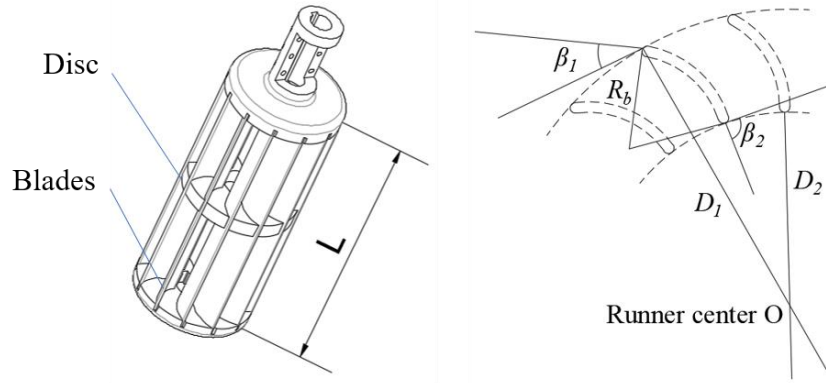


Fig.5 The main geometrical parameters of the cross-flow runner

Table 1 The values of runner main geometrical parameters

| Geometrical Parameters | Symbols | Values |
|-----------------------------------|-----------|------------|
| Blade outer angle | β_1 | 39° |
| Blade inner angle | β_2 | 90° |
| Outer diameter | D_1 | 98mm |
| Inner diameter | D_2 | 66mm |
| Ratio of inner and outer diameter | D_2/D_1 | 0.68 |
| Blade radius | R_b | 18.2mm |
| Blades number | N_b | 20 |
| Runner length | L | 215mm |

2.2. Numerical approach

CFD simulation has been demonstrated an effective and promising method for hydro turbine design [26] and performance prediction [27, 28]. In this study, the CFD method is used to study the effects of different block design on the turbine performance.

2.2.1 Grids generation

After geometrical design, the physical model of the proposed inline turbine was built in SolidWorks 2014, which is a powerful 3D computer-aided design software, then the model was imported in ANSYS ICEM 14.5 for meshing. The physical model is composed of four main parts: inlet extension part, turbine body, runner and outlet

extension part, general grid interface is used to connect these parts. The whole computational domain is divided into two main domains: stationary domain and rotating domain. The stationary domain composed of inlet extension part, turbine body and outlet extension part and the rotating domain consisting of the runner. The geometries of turbine body and runner are highly complex because of the curved walls and narrow tip regions, so in the meshing process, the “tetra mesh” was employed to generate grids in the domains far from boundaries, while the “prism mesh” was used for grid generation in the domains near boundaries, i.e. the pipe wall and blades. Such strategy could achieve a good balance between calculation time and accuracy. To minimize the numerical uncertainty in the solution, a grid independence test was conducted considering the output shaft power at the runner rotating speed of 35rad/s. Four meshing schemes were tested and their grid numbers are 1.82, 2.88, 3.77 and 5.31 million, respectively. Figure 6 shows the grid independence test results, according to the results, the total grid number of 3.77 million was taken for the next study. As shown in Figure 7 is the final computational mesh, which is divided into two symmetric parts but only one was modeled and simulated, assuming an impermeable boundary along the symmetry plane.

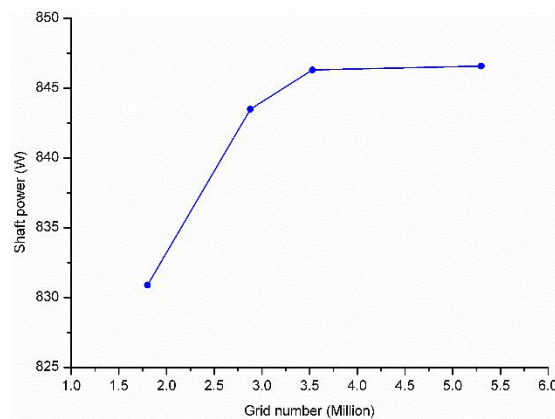


Fig.6 Grid independence test results

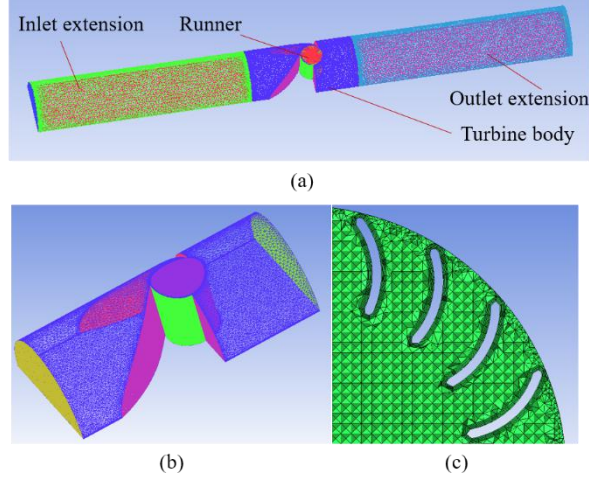


Fig.7 The final meshing scheme (a) meshing of whole computational domain (b) meshing of the turbine body (c) zoom view of the blades meshing

2.2.2 Governing equation and turbulence model

The incompressible isothermal flow through a turbomachine is fully described by the continuity and momentum equations, which are called the Navier-Stokes equations and written as:

$$\frac{\partial u_i}{\partial x_i} = 0 \quad (14)$$

$$\frac{\partial u_i}{\partial t} + u_j \frac{\partial u_i}{\partial x_j} = -\frac{1}{\rho} \frac{\partial p}{\partial x_i} + \nu \frac{\partial^2 u_i}{\partial x_i \partial x_j} \quad (15)$$

where u is the velocity, p is the pressure, ν is the kinematic viscosity of fluid, ρ is the density of fluid.

Since solving the Navier-Stokes equations is computationally expensive for high Reynolds number flows in complex geometries, the Reynolds averaged Navier-Stokes (RANS) equations are generally solved to determine the mean velocity field. RANS equations are obtained by time-averaging the Navier-Stokes equations for the mean values of the flow variables over a sufficiently long period compared to the frequencies of turbulent fluctuations, and are written as:

$$\frac{\partial u_i}{\partial x_i} = 0 \quad (16)$$

$$\frac{\partial U}{\partial t} + U_j \frac{\partial U_i}{\partial x_j} = -\frac{1}{\rho} \frac{\partial P}{\partial x_i} + \frac{\partial}{\partial x_j} \left[\nu \left(\frac{\partial U_j}{\partial x_i} + \frac{\partial U_i}{\partial x_j} \right) - \overline{u'_i u'_j} \right] \quad (17)$$

where U is the time-averaged velocity, u'_i is the fluctuating velocity due to turbulence and $-\overline{\rho u'_i u'_j}$ is the Reynolds shear stress.

RANS simulations with appropriate turbulence models have been widely used for turbomachinery design analyses due to their low computational cost and satisfactory predictive capability for average device performance [29]. Several turbulence models were proposed to close the RANS equations, e.g. standard $k-\varepsilon$ model, RNG $k-\varepsilon$ model, $k-\omega$ model and SST $k-\omega$ model. Among them, $k-\omega$ model is used because the SST $k-\omega$ model combines the standard $k-\omega$ model and standard $k-\varepsilon$ model, it takes the effects of turbulence shear stress into consideration in the definition of the turbulence viscosity and could capture the micro flow in the viscous layer. Besides, in the reference [30], the author conducted several turbulence models in CFD simulation of cross-flow turbine design, the results showed that the SST $k-\omega$ model can be reliable and accurate in numerical study of cross-flow turbines. So in this study, the SST $k-\omega$ model is chose for numerical simulation.

2.2.3 Boundary conditions

The simulations were conducted in ANSYS Fluent 14.5 using a second-order-accurate finite-volume discretization scheme and the target RMS is set to 10^{-5} . The inlet and outlet boundary conditions are determined based on the working conditions in the water mains. As the flow velocity and water head are the main parameters for turbine design and the water head on the turbine downstream is an important issue assessing the influence of turbine application on normal water supply. So the inlet velocity is considered as the inlet boundary condition of the inlet face while the outlet boundary condition is set as pressure outlet. Besides, the boundary condition of turbine wall,

blocks and blades is set as non-slip smooth wall.

2.3 Experimental setup and prototype

In our previous research, a preliminary inline cross-flow turbine was developed by numerical method and its prototype was manufactured and tested in a hydraulic test rig. Figure 8 shows the scheme and prototype of the preliminary turbine. As can be seen in Figure 8, a guide block with concave surface and a plate conversion block are used to direct the water flow and accelerate flow velocity. Besides, the guide block is designed to decrease the water resistance which exerts on the returning blades. Figure 9 shows the structure of the hydraulic test rig which was built based on a carbon contact chamber at Ma On Shan Water Treatment Works (MOSWTW) of Hong Kong. The test rig is mainly composed of two parallel submersible pumps, DN250 water pipes, the water turbine, two pressure meters, a flow meter, an adjustable ball valve and a frequency converter controller. Among them, the submersible pumps are used to provide water flow with maximum flow velocity of 3m/s and water head of 80m water in DN250 water pipes. The frequency converter controller is used to regulate pump working speed. By adjusting working frequency of the submersible pumps and opening degree of the ball valve, different flow velocity and water head can be achieved in the test rig. To transfer the torque from runner into electricity, a 24V three-phase permanent magnet alternating generator with low starting torque is adopted. Besides, two pressure meters are used to examine the pressure drop between the upstream and downstream of the water turbine. In the experimental process, data about the flow velocity, charging voltage and current, water head of upstream and downstream can be transmitted and recorded in a monitoring computer.

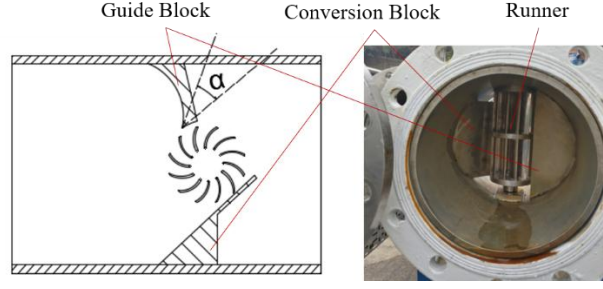


Fig.8 Scheme and product of the preliminary turbine

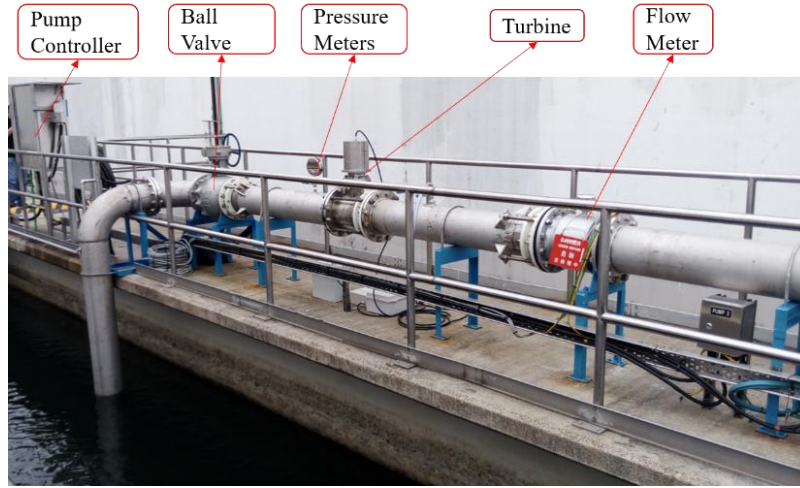


Fig.9 The hydraulic test rig

2.4 Data analysis

This study aims to investigate the effects of different block design on the turbine performance mainly by numerical method. In the simulation process, the water head at the inlet and outlet boundary and the torque of the runner are recorded for turbine performance assessment. The simulated performance parameters including water head loss ΔH , output shaft power P_{sout} , input power P_{sin} and turbine efficiency η can be calculated by the followed equations:

$$\Delta H = H_{in} - H_{out} \quad (18)$$

$$P_{sout} = T\omega \quad (19)$$

$$P_{sin} = \rho g \Delta H Q \quad (20)$$

$$\eta = \frac{P_{out}}{P_{in}} \quad (21)$$

where H_{in} is the water head at inlet boundary, m; H_{out} is the water head at outlet boundary, m; ω is the rotational speed, rad/s; T is the torque of the runner, N·m; ρ is water density, kg/m³; g is acceleration of gravity, m/s²; Q is the water volume flow rate, m³/s.

Besides, the recorded experimental output power is the power generated by the generator. But in the process of power converting and transferring, losses such as mechanical loss and generator conversion loss are inevitable, so the experimental output shaft power P_{out} should be obtained as:

$$P_{out} = P_{gen} / \eta_{me} \eta_g \quad (22)$$

where P_{gen} is the power generated by the generator, W; η_{me} is the overall mechanical efficiency, and η_g is the conversion efficiency of generator. In this study, the mechanical efficiency and generator conversion efficiency are determined based on the data provided by parts suppliers.

Tip speed ratio (TSR), which means the ratio of the peripheral speed of the turbine runner and the flow velocity and expressed by Equation (23), is an important parameter related to turbine efficiency. To analyze the effect of TSR on turbine performance, the runner rotation speed was varied in different CFD simulations.

$$TSR = \frac{r\omega}{V} \quad (23)$$

where r is the runner radius (m); V is the flow velocity (m/s).

3. Results and analysis

CFD simulation has been proved a relatively effective way in performance prediction and flow field analysis of cross-flow turbines [17, 18, 22]. In this study, a series of

simulations were conducted to understand the function of the block and the effects of different block design on turbine performance.

3.1 Validation of the CFD model

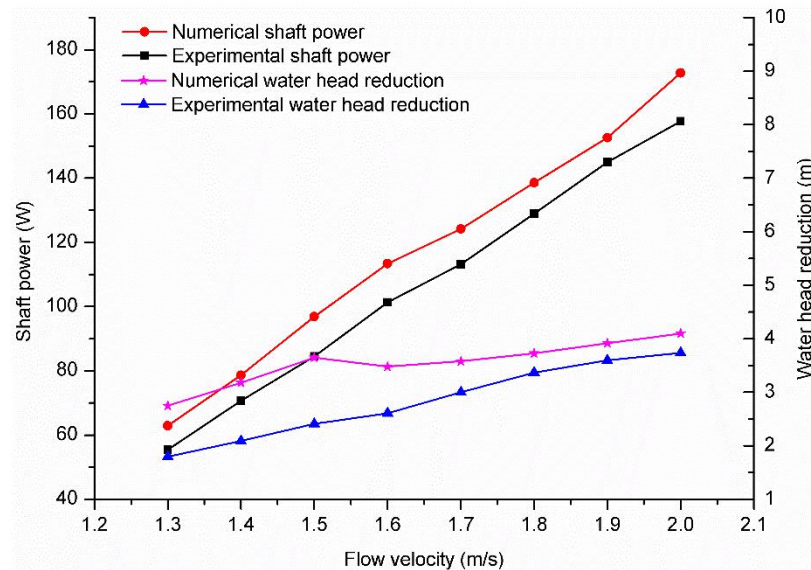


Fig.10 The comparison between numerical and experimental results

A physical model of the turbine prototype mentioned above was built and its performance at different flow velocity was simulated using the described numerical method. Besides, the corresponding experimental performance was obtained in the hydraulic test rig. The comparison between numerical and experimental results is shown in Figure 10. It can be observed that the tendencies of numerical and experimental results agree very well, both the numerical and experimental shaft power and water head reduction increase gradually with the increment of flow velocity. However, some deviations exist between the experimental and numerical results. Two main reasons may account for the difference. Firstly, the CFD model is simplified, resulting in calculation uncertainties which are very difficult to be measured and ruled out. On the other hand, the mechanical loss caused by the mechanical seals and the conversion loss of the generator cannot be estimated accurately. As water pressure in urban water supply pipes is very high, the actual mechanical loss is higher than that provided by the supplier. Besides, the generator cannot always operate under the best

working condition, resulting in a lower conversion efficiency. Most of the error percentages in terms of shaft power are limited in 10% and the error values of water head reduction are all less than 1m water. Hence, the proposed numerical method is suitable for performance analysis of the inline turbine regardless of some acceptable errors.

3.2 Output power and efficiency

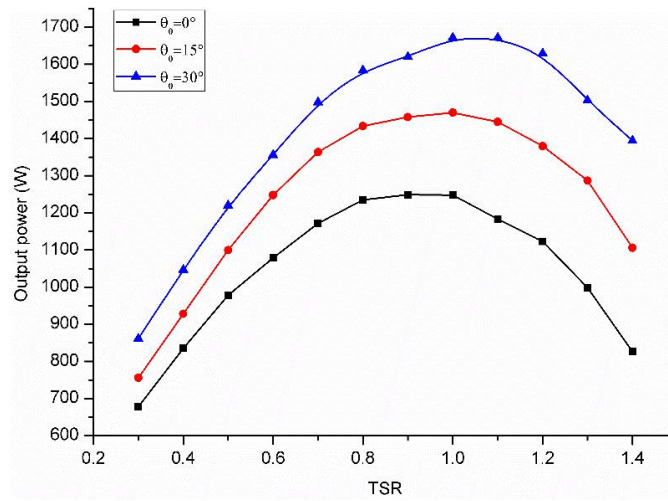


Fig.11 Output power of inline turbine with different blocks

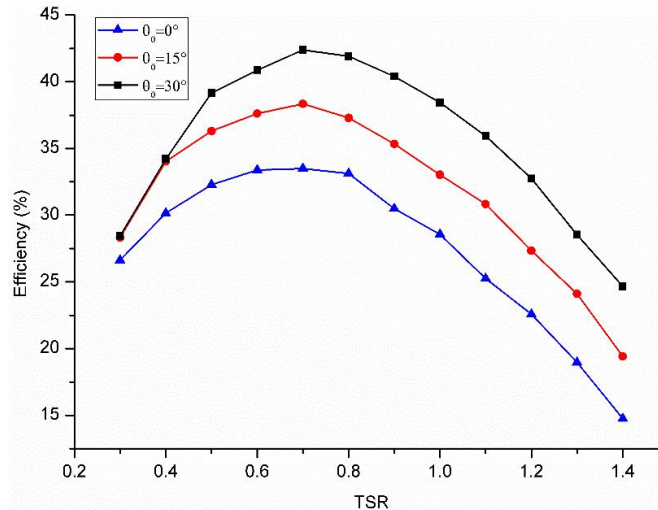


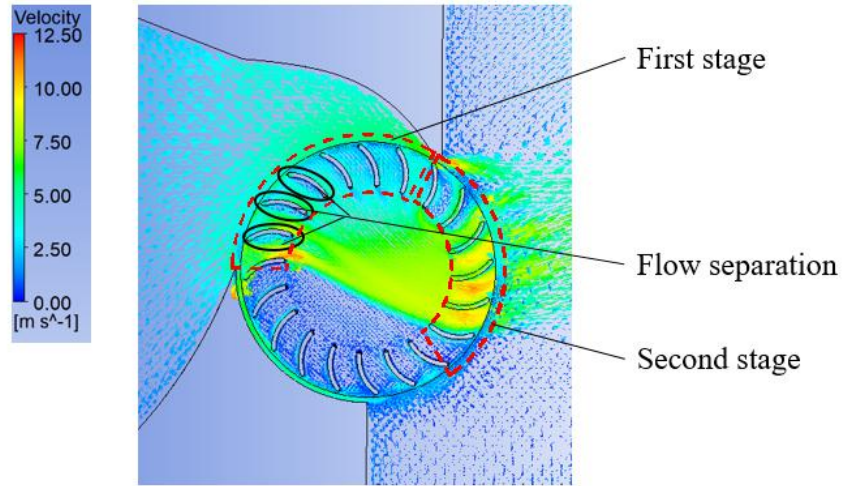
Fig.12 Efficiency of inline turbine with different blocks

To investigate the effects of different block shape on turbine performance, three turbine models with different guide block orientation angles were built and simulated at the inlet velocity of 1.5m/s, which is indicated by the Water Supplies Department as

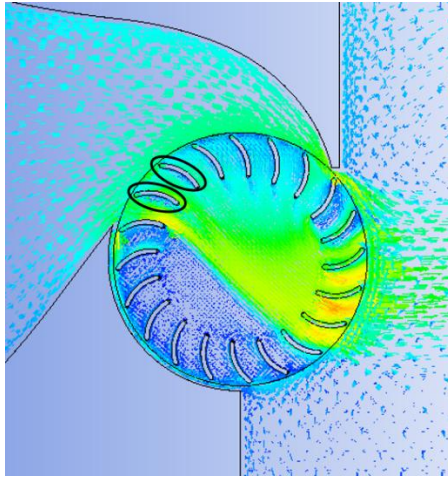
the average flow velocity inside water mains. The output power and efficiency of three different models are indicated in Figure 11 and Figure 12, respectively. It is clear that both the output power and efficiency increase with the increment of TSR until reach the maximum values, then decrease. In terms of output power, the maximum value of model with $\theta_0 = 0^\circ$ occurs when TSR equals to 0.9 while the other two models get the maximum output power at the TSR of 1. It can also be observed that with the increase of θ_0 , the maximum output power also increases significantly. For example, the maximum output power of model with $\theta_0 = 30^\circ$ increases by 422W (nearly 35%) compared to the model with $\theta_0 = 0^\circ$. From the aspect of efficiency, the variation tendency is similar to that of output power. But the best efficiency of all the models occurs at TSR of 0.7. Among the three models, the model with $\theta_0 = 30^\circ$ has a better efficiency than other two models and its best efficiency is 42.4%. In conclusion, the orientation angle of guide block does have an impact on the turbine output power and efficiency, the reasons that account for the difference will be analyzed in the followed parts.

3.3 Flow characteristics

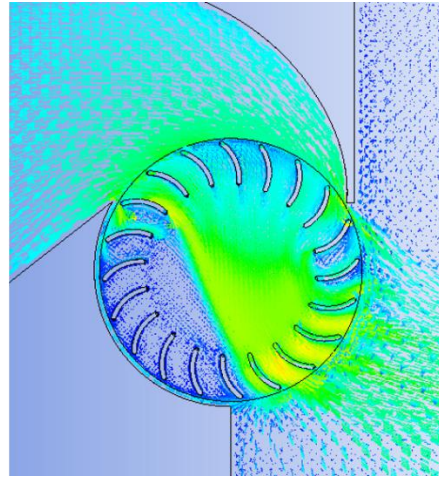
To investigate the reasons for performance difference of the three models, flow characteristics which play important roles in determining turbine performance are analyzed. In this study, the flow velocity vectors in domains of block and runner and the flow velocity and angle at runner inlet are emphasized. Figure 13 indicates the flow velocity vectors of three models at TSR of 0.7. In all the models, the block can improve the flow velocity through the runner, which means the block can increase kinetic energy of water flow. Besides, the flow velocity in the second stage is higher than that in the first stage, this is because the blades passages in the first stage are converging and water flow accelerates before entering in the blades passages of the second stage.



(a) $\theta_0 = 0^\circ$



(b) $\theta_0 = 15^\circ$



(c) $\theta_0 = 30^\circ$

Fig.13 Flow velocity vectors of three models at TSR of 0.7

The ideal flow through the runner of a cross-flow turbine is expected to be parallel to the blade surface, however, it can be noticed that in Figure 13(a) and Figure 13(b), flow separations occur in the first stage of model with $\theta_0 = 0^\circ$ and $\theta_0 = 15^\circ$. Flow separation is caused by the mismatching between flow attack angle and blades inlet angle and has a negative impact on turbine performance. The flow separation can not only cause hydraulic loss, but also have a negative influence on the quality of water flow of the second stage [30]. Compared to the other models, the model with $\theta_0 = 30^\circ$ has a better flow field and only slight flow separation occurs in the blades

passages. The main reason for this phenomenon is that the guide block of model with $\theta_0 = 30^\circ$ covers more area of the runner and has a better function in directing the water flow, leading to a better matching between the flow attack angle and the blades inlet angle. It can also be observed that there is no flow separation in the second stage of all the three models, this is because the flow velocity at the entrance of second stage is slightly increased due to the converging blades passages in the first stage.

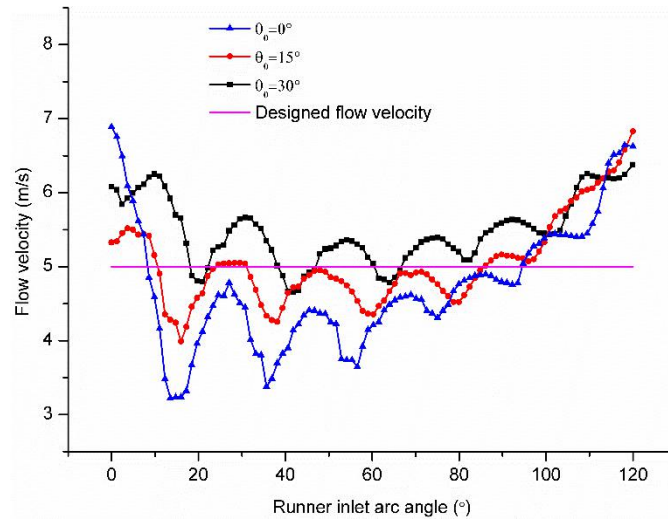


Fig.14 Computed and designed flow velocity along the runner inlet arc

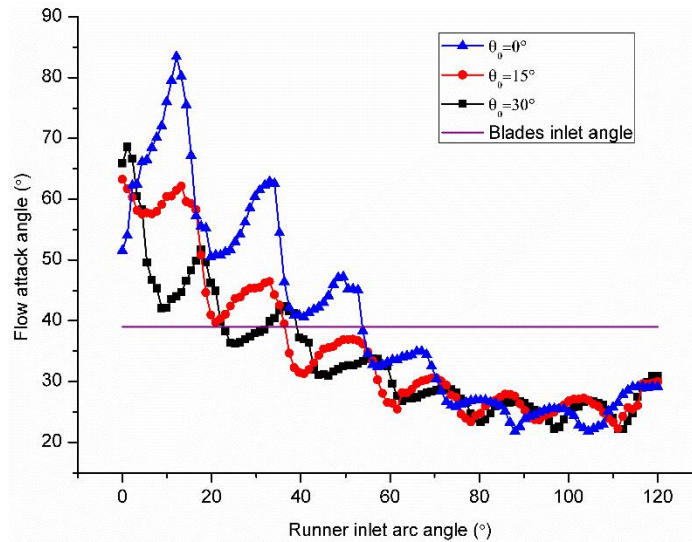


Fig.15 Computed flow attack angle along the runner inlet arc

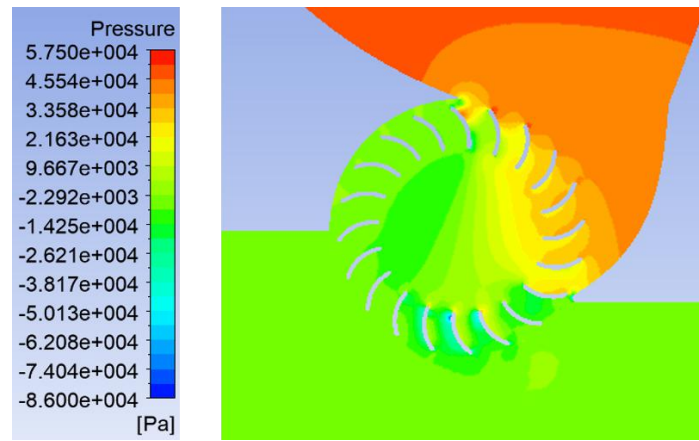
The computed and designed flow velocity distribution along the runner inlet is shown in Figure 14. Note that, the designed flow velocity is determined based on the

hypothesis that the conversion block transfers all the water head into flow kinetic energy, which is expressed by Equation (4). It is obvious in Figure 14 that the computed flow velocity of all the three models fluctuate sharply along the runner inlet arc. At the initiating of the runner inlet, the flow velocity is relatively high, this is possibly because the initiating of the runner inlet is also the terminal of guide block, where jet flow is easily formed. It can be observed that in the angle range from 20° to 90° of runner inlet arc, the flow velocity of the model with $\theta_0 = 30^\circ$ fluctuates around the designed flow velocity, which means the conversion block can convert nearly all the reduced water head into flow kinetic energy and fulfill its intended functions. The flow velocity of the model with $\theta_0 = 15^\circ$ and $\theta_0 = 0^\circ$ in the same runner inlet arc angle range are all less than the designed flow velocity, this is because the runner inlet areas covered by conversion block in these two models are relatively small, as a result, the conversion block cannot fully achieve its function. It is interesting to note that at the terminal of runner inlet, the flow velocity of all the three models increases sharply. The main reason for this phenomenon is the exist of tip clearance between conversion block and runner and leakage through the tip clearance may accelerate the flow velocity.

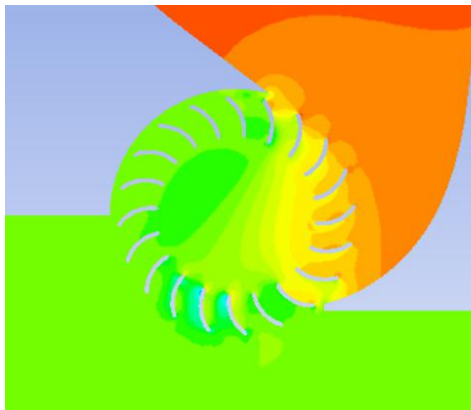
Figure 15 shows the computed flow attack angle along the runner inlet and the blades inlet angle. As indicated in the figure, there is significant difference between the computed attack angle and blades inlet angle, especially in the angle range from 0° to 40° of runner inlet arc. Comparing these three models, the difference in models with $\theta_0 = 15^\circ$ and $\theta_0 = 0^\circ$ is greater than that in the model with $\theta_0 = 30^\circ$, which explains the existence and variation of flow separations indicated in Figures 13. Besides, it can be observed that the difference decreases with the increase of θ_0 , which results from the fact that the guide block in models with bigger θ_0 can cover more runner inlet area that towards flow direction and have a better function in

directing the water flow. In the angle range from 60° to 120° of runner inlet arc, the attack angle of all the three models keeps stable around 26° , which is much smaller than the blades inlet angle. To further enhance the inline turbine performance, it is suggested to improve the blades design for a better matching with the proposed block design, and this investigation will be addressed in a subsequent paper.

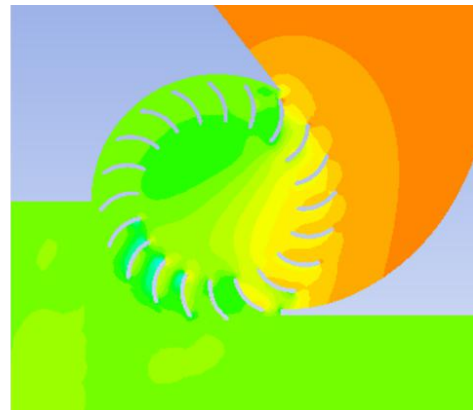
3.4 Pressure distribution



(a) $\theta_0 = 0^\circ$



(b) $\theta_0 = 15^\circ$



(c) $\theta_0 = 30^\circ$

Fig.16 Pressure contours of three models at TSR of 0.7

The pressure contours in the flow field of conversion block and runner of three models are shown in Figure 16. In all the three models, the blocks can function as a convergence nozzle while the downstream side can function as a diffuser. The water pressure at the upstream side of runner is higher than that on the downstream side,

leading to a pressure difference which can draw in more water and increase the flow velocity. Usually, the runner blades rotate from pressure side to suction side because of the force of water from pressure side. However, it can be observed that small high-pressure regions occur at the leading edge of suction side of the beginning several blades at the first stage of all the three models, which has a negative impact on runner torque output. Comparing pressure contours of three models, high pressure regions shrink with the increase of θ_0 because the guide block's function of directing water flow is significantly enhanced with the increment of θ_0 . Pressure difference exists between pressure side and suction side of the remaining blades at the first and second stage, leading to normal torque output of the runner. The torque output of each blade at the first and second stage is illustrated in Figure 17. The torque output of the beginning three blades at the first stage is negative or very small, which is consistent with the pressure distribution in Figure 16. After that, the torque extraction of blades experiences a significant increase. Among the three models, the model with $\theta_0 = 30^\circ$ possesses a good performance in blades torque extraction.

Figure 18 compares the torque output of the first and second stage. It is clear that in the three different models, the torque output in the second stage is similar and is higher than that in the first stage, this is mainly due to the followed reasons: Firstly, the flow attack angle has a good matching with the blade inlet angle at the second stage and no flow separation is found in the blades passages. Secondly, the water flow accelerates slightly before entering the second stage because the converging blades passages in first stage. Besides, the torque output at first stage nearly doubles when θ_0 increases from 0° to 30° , which is mainly because that in the model with bigger θ_0 , the guide block has a better function of reducing high pressure regions on blades suction side while the conversion block can convert more water head into kinetic energy.

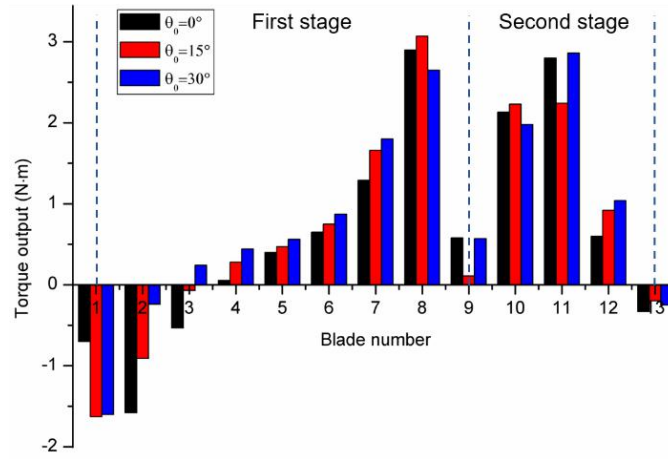


Fig.17 Torque output of each blade at the first and second stage

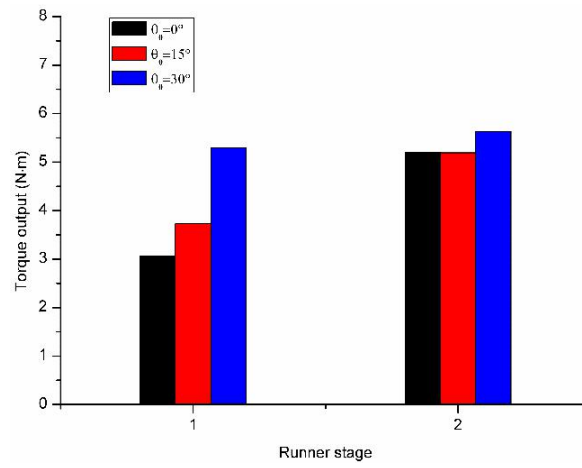


Fig.18 Torque output of different stage

3.5 Water head reduction

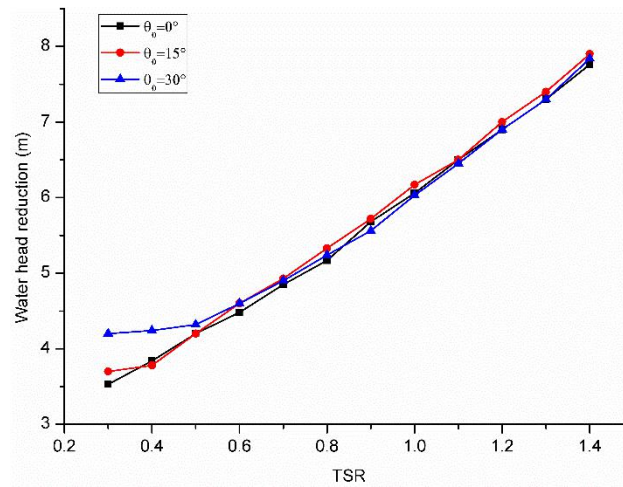


Fig.19 Water head reduction of three models

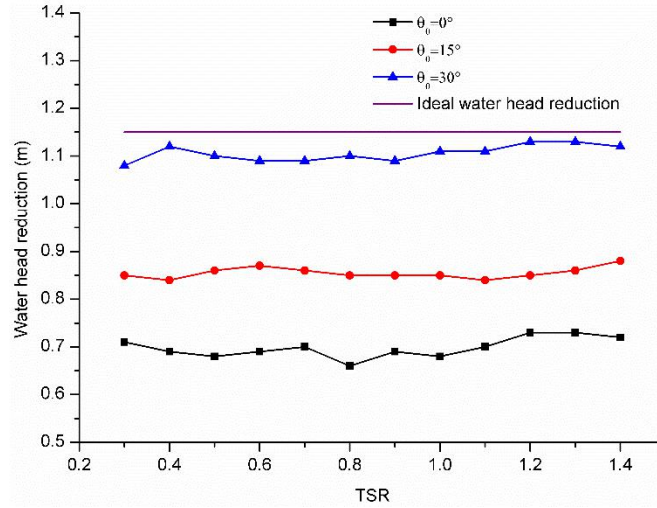


Fig.20 Water head reduction caused by the conversion block

Water head reduction is one of the major considerations when applying hydro turbines in water mains because excess water head loss will influence normal water supply. The numerical water head reduction of three models is shown in Figure 19 which indicates that these three models have similar performance in water head reduction. At the best efficiency TSR, that is 0.7, the water head reduction of three models are all less than 5m water. As suggested by the Water Supplies Department of Hong Kong, 5m water head reduction is within the acceptable range [12]. To further study the function of proposed block, the water head reduction caused by the conversion block is illustrated in Figure 20. It is assumed that the water head loss caused by friction or shock loss can be ignored, so the water head reduction in conversion block all converted into kinetic energy. As shown in Figure 20, the water head reduction caused by conversion block in models with $\theta_0 = 0^\circ$, $\theta_0 = 15^\circ$ and $\theta_0 = 30^\circ$ are around 0.7, 0.85 and 1.1m water, respectively, while the ideal value should be 1.15m water. The results further demonstrate the better performance of the inline turbine model with $\theta_0 = 30^\circ$.

Conclusion

In this study, an inline cross-flow turbine is newly developed for hydropower generation from urban water mains using limited water head. The proposed inline

turbine can be used for continuous power supply to the water monitoring sensors and meters which are widely used in the water supply system worldwide. Application of the developed turbine can significantly reduce the battery use and ensure reliable and constant power to water monitoring devices, thus durable monitoring on water leakage and quality can be ensured. Specifically, this research proposes a block design method for inline cross-flow turbines used in water supply mains. Besides, the effects of different block design on the turbine performance is studied by numerical method. The output power, efficiency, flow field characteristics and water head reduction have been analyzed to verify the proposed method and analyze the function of the blocks. As referred from the present study, the following conclusions can be obtained:

- (1) The proposed design method is effective for inline cross-flow turbine design. Numerical results showed that the inline turbine could reach its maximum efficiency of 42.4% with about 1500W power output.
- (2) The blocks play an important role in performance enhancement of inline cross-flow turbines because the blocks can convert part of the water head into kinetic energy, leading to a high flow velocity through the runner.
- (3) The improvement of pressure distribution inside the inline turbine is considerable by improving the block design. The high-pressure regions on the suction side of the beginning several blades at the first stage can be reduced obviously and the torque output of the first stage nearly doubles after the block improvement.
- (4) Numerical results showed that the proposed inline turbine can be applied in water mains without influencing normal water supply as the water head reduction through the turbine is within the acceptable range.
- (5) Comparing the models with $\theta_0 = 0^\circ$, $\theta_0 = 15^\circ$ and $\theta_0 = 30^\circ$, model with $\theta_0 = 30^\circ$ has a better performance than other two models. This is because in this model, the blocks can not only reduce negative torques at the runner first stage, but

also convert more water head into kinetic energy.

(6) The research results could provide guidance for the on-site application of inline cross-flow turbines. Based on different working condition (i.e. flow rate, water head and power demand), the block shape can be determined accordingly, which significantly contribute to the turbine's widespread use around the world.

Acknowledgement

The authors would appreciate the financial supports provided by the Innovation and Technology Fund of Hong Kong Special Administrative Region Government (Grant No.: ITS/032/13) and the help from the Water Supplies Department of the Hong Kong SAR Government.

Reference

- [1] Huang, Weilong, Ding Ma, and Wenying Chen. "Connecting water and energy: assessing the impacts of carbon and water constraints on China's power sector." *Applied Energy* 185 (2017): 1497-1505.
- [2] Wang, Saige, Tao Cao, and Bin Chen. "Urban energy–water nexus based on modified input–output analysis." *Applied energy* 196 (2017): 208-217.
- [3] Xu, Qiang, et al. "Review on water leakage control in distribution networks and the associated environmental benefits." *Journal of Environmental Sciences* 26.5 (2014): 955-961.
- [4] Cheung, C. T., K. W. Mui, and L. T. Wong. "Energy efficiency of elevated water supply tanks for high-rise buildings." *Applied energy* 103 (2013): 685-691.
- [5] Operation and Maintenance of Waterworks, Water Supplies Department, Hong Kong.
<http://www.wsd.gov.hk/en/core-businesses/operation-and-maintenance-of-waterworks/index.html>
- [6] Abegaz, Brook W., Tania Datta, and Satish M. Mahajan. "Sensor technologies for the energy-water nexus—a review." *Applied Energy* 210 (2018): 451-466.
- [7] Mehajabin N, Razzaque M A, Hassan M M, et al. Energy-sustainable relay node deployment in wireless sensor networks. *Computer Networks*, 2016, 104: 108-121.
- [8] Valera A C, Soh W S, Tan H P. Enabling sustainable bulk transfer in environmentally-powered wireless sensor networks. *Ad Hoc Networks*, 2017, 54: 85-98.
- [9] Rosenbloom D, Meadowcroft J. Harnessing the Sun: Reviewing the potential of solar photovoltaics in Canada. *Renewable and Sustainable Energy Reviews*, 2014, 40: 488-496.
- [10] Weimer M A, Paing T S, Zane R A. Remote area wind energy harvesting for low-power autonomous sensors. *system*, 2006, 2(1): 2.
- [11] Myers R, Vickers M, Kim H, et al. Small scale windmill. *Applied Physics Letters*, 2007, 90(5): 054106.
- [12] Chen J, Yang H X, Liu C P, et al. A novel vertical axis water turbine for power generation from water pipelines. *Energy*, 2013, 54: 184-193.
- [13] Ma T, Yang H, Guo X, et al. Development of inline hydroelectric generation system from municipal water pipelines[J]. *Energy*, 2018, 144: 535-548.
- [14] Adhikari R C, Wood D H. A new nozzle design methodology for high efficiency cross-flow hydro turbines. *Energy for Sustainable Development*, 2017, 41: 139-148.
- [15] Sammartano V, Aricò C, Carravetta A, et al. Banki-Michell optimal design by computational fluid dynamics testing and hydrodynamic analysis. *Energies*, 2013, 6(5): 2362-2385.
- [16] Choi Y D, Lim J I, Kim Y T, et al. Performance and internal flow characteristics of a cross-flow hydro turbine by the shapes of nozzle and runner blade. *Journal of Fluid Science and Technology*, 2008, 3(3): 398-409.

- [17]Chichkhede S, Verma V, Gaba V K, et al. A Simulation Based Study of Flow Velocities across Cross Flow Turbine at Different Nozzle Openings. *Procedia Technology*, 2016, 25: 974-981.
- [18]Acharya N, Kim C G, Thapa B, et al. Numerical analysis and performance enhancement of a cross-flow hydro turbine. *Renewable energy*, 2015, 80: 819-826.
- [19]Elbatran A H, Ahmed Y M, Shehata A S. Performance study of ducted nozzle Savonius water turbine, comparison with conventional Savonius turbine. *Energy* 2017.
- [20]Prasad D D, Ahmed M R, Lee Y H. Flow and performance characteristics of a direct drive turbine for wave power generation. *Ocean Engineering*, 2014, 81: 39-49.
- [21]Kim K P, Ahmed M R, Lee Y H. Efficiency improvement of a tidal current turbine utilizing a larger area of channel. *Renewable energy* 2012, 48: 557-564.
- [22]Elbatran A H, Yaakob O B, Ahmed Y M, et al. Novel approach of bidirectional diffuser-augmented channels system for enhancing hydrokinetic power generation in channels. *Renewable Energy*, 2015, 83: 809-819.
- [23]Mockmore C A, Merryfield F. The Banki water turbine. 1949.
- [24]Aziz N M, Totapally H G S. Design Parameter refinement for improved Cross-Flow turbine performance. *Engineering Report*, 1994.
- [25]Aziz N M, Desai V R. A laboratory study to improve the efficiency of cross-flow turbines. *Engineering Report*, 1993.
- [26]Williamson S J, Stark B H, Booker J D. Performance of a low-head pico-hydro Turgo turbine. *Applied Energy*, 2013, 102: 1114-1126.
- [27]Du J, Yang H, Shen Z, et al. Micro hydro power generation from water supply system in high rise buildings using pump as turbines. *Energy*, 2017, 137: 431-440.
- [28]Benzon D S, Aggidis G A, Anagnostopoulos J S. Development of the Turgo Impulse turbine: Past and present. *Applied energy*, 2016, 166: 1-18.
- [29]Gourdain N. Prediction of the unsteady turbulent flow in an axial compressor stage. Part 1: Comparison of unsteady RANS and LES with experiments. *Computers & Fluids*, 2015, 106:119-129.
- [30]Adhikari R. Design Improvement of Cross-flow Hydro Turbine[D]. University of Calgary, 2016.